Integrated MIMO Signal Design via Spatio-Spectral Modulation

1st Xianxiang Yu
School of Information and Communication Engineering
University of Electronic Science and Technology of China
Chengdu, China
xianxiangyu@uestc.edu.cn

2nd Xue Yao
School of Information Science and Engineering
Southeast University
Nanjing,China
yaoxue_2016@163.com

3rd Hui Qiu
School of Information and Communication Engineering
University of Electronic Science and Technology of China
Chengdu, China
202021010915@std.uestc.edu.cn

4th Guolong Cui
School of Information and Communication Engineering
University of Electronic Science and Technology of China
Chengdu, China
cuiguolong@uestc.edu.cn

***Abstract*—This paper considers the integrated waveform design to simultaneously achieve a desired radar beampattern and multi-users communication for a dual-function Multiple-Input Multiple-Output (MIMO) system. To this end, a spatio-spectral modulation strategy via shaping the spatial waveform Energy Spectral Density (ESD) in directions of communication is proposed for the communication function, while beampattern Integrated Sidelobe Level (ISL) is minimized to enhance radar detectability. Meanwhile, Peak-to-Average Ratio (PAR) and power restrictions to comply with the current hardware technique and the mainlobe width constraint to cohere the beampattern main energy on the spatial region of interest are forced, respectively. Finally, numerical results highlight the effectiveness of both the proposed dual function scheme and the waveform synthesis technique.**

***Index Terms*—Dual-Function MIMO radar Communication System; Beampattern Integrated Sidelobe Level (ISL); Multi-Users Communication;**

I. Introduction

Recently, Dual Function Radar Communication (DFRC) system sharing hardware and signal processing modules in an integrated system instead of two separated systems, has attracted significant attention [1]. Herein, the design of the integrated waveform to simultaneously implement radar and communication is the key technology of DFRC system. The existing DFRC waveform design methods can be divided into two main categories: communications waveform-based approaches and radar waveform-based schemes. The latter is concerned in this paper.

The ambiguity function sidelobe nulling and the spectral nulling modulations are proposed to embed communication information [2], [3]. Some other interesting modulation methods including beampattern sidelobe level and phase modulation, frequency agile with random antenna allocation for phased array are studied [4]–[6]. However, a typical phased-array radar transmits the appropriately phase-shifted counterpart of a single waveform via each antenna thus failing to exploit waveform diversity for achieving the dual-function.

MIMO radar system allowing the improved Degrees-of-Freedom (DoFs) on waveform diversity to achieve the dual-function has become a hot research territory. In [7], MIMO radar beampattern is devised using a linear combination of orthogonal waveforms, while the information bits are conveyed by the permutation of orthogonal waveform cluster. However, the waveform Peak-to-Average Ratio (PAR) is not directly controlled leading to low transmit power efficiency. In [8], the correlated Frequency Hopping MIMO (FH-MIMO) radar waveforms that enable appropriately controlling the beampattern as well as improving data rate using phase modulation is synthesized. In [9], the communication data rate is significantly enhanced via an extended signal strategy involving beampattern amplitude and phase, spatial spectrum, and array configuration, while the desired MIMO radar beampattern is shaped through emitting a linear combination of the FH orthogonal waveforms but with high PAR. Furthermore, [10] mainly focus on the beampattern optimization under waveform constraints and communication performance restriction assuming that the information has been embedded in the integrated waveform.

In this paper, we still focus on the design of the integrated waveform to simultaneously implement MIMO radar detection and communication. In a departure from most existing modulation approaches, we provide a novel perspective from controlling the waveform spatio-spectral energy to accomplish multi-users communication.

II. System Model

Consider that a colocated narrow band dual-function MIMO radar communication system with N transmit antennas is

This work was supported in part by the National Natural Science Foundation of China under Grants 62101097, U19B2017, 61871080 and 61701088, by ChangJiang Scholar Program, by the 111 project No.B17008, by China Postdoctoral Science Foundation under Grants 2020M680147 and 2021T140096.

surveilling the space of interest, while delivering communication information to C communication multi-users.

Assume that each transmitting antenna emits a distinct waveform $\boldsymbol{s}_n(m), n = 1, 2, \cdots, N$, $m = 1, 2, \cdots, M$, with M the number of samples in each transmitting pulse. Let us denote by $\bar{\boldsymbol{s}}_m = [\boldsymbol{s}_1(m), \boldsymbol{s}_2(m), \cdots, \boldsymbol{s}_N(m)]^T \in \mathbb{C}^N$, the m-th sample of N waveforms. The signal arriving at the target azimuth θ can be written as $\boldsymbol{x}(m) = \boldsymbol{a}^\dagger(\theta)\bar{\boldsymbol{s}}_m$, where $\boldsymbol{a}(\theta)$ denotes the transmit spatial steering vector. In particular, for the Uniform Linear Arrays (ULAs), it is given by $\boldsymbol{a}(\theta) = [1, e^{j2\pi\frac{d_T}{\lambda}\sin\theta}, \cdots, e^{j2\pi\frac{d_T}{\lambda}(N-1)\sin\theta}]^T$ with d_T and λ the array inter-element spacing of the transmitter and wavelength, respectively. Hence, the power of transmitted signal at azimuth θ can be computed as

$$\begin{aligned}\frac{1}{M}\sum_{m=1}^{M}\|\boldsymbol{a}^\dagger(\theta)\bar{\boldsymbol{s}}_m\|^2 &= \frac{1}{M}\sum_{m=1}^{M}\bar{\boldsymbol{s}}_m^\dagger\boldsymbol{a}(\theta)\boldsymbol{a}^\dagger(\theta)\bar{\boldsymbol{s}}_m \\ &= \frac{1}{M}\|(\boldsymbol{I}_M \otimes \boldsymbol{a}^\dagger(\theta))\boldsymbol{s}\|^2 = \boldsymbol{s}^\dagger\boldsymbol{A}(\theta)\boldsymbol{s},\end{aligned} \tag{1}$$

where $\boldsymbol{s} = \text{vec}\{[\boldsymbol{s}_1, \boldsymbol{s}_2, \cdots, \boldsymbol{s}_N]^T\} \in \mathbb{C}^{NM}$ and $\boldsymbol{A}(\theta) = \frac{1}{M}\boldsymbol{I}_M \otimes (\boldsymbol{a}(\theta)\boldsymbol{a}^\dagger(\theta))$.

Next, we will propose a new information embedding and demodulation strategy.

A. Information Embedding via Spatio-Spectral Modulation

We propose an information embedding approach based on spatio-spectral passbands and stopbands. Specifically, we assume that the DFRC system communicate with C users located at azimuth $\varphi_c, c = 1, \cdots, C$, respectively. The spatially synthetic far field baseband discrete signal $\boldsymbol{x}_c \in \mathbb{C}^M$ toward to azimuth φ_c can be written as (ignoring the propagation path loss)

$$\boldsymbol{x}_c = \boldsymbol{S}\boldsymbol{a}^*(\varphi_c), \tag{2}$$

where $\boldsymbol{S} = [\boldsymbol{s}_1, \boldsymbol{s}_2, \cdots, \boldsymbol{s}_N] \in \mathbb{C}^{M\times N}$.

A normalized frequency band $\Omega \in [0, 1)$ is occupied by $\boldsymbol{x}_c, c = 1, \cdots, C$, with L frequency bands $\Omega_l = (f_{l,1}, f_{l,2}) \in \Omega, l = 1, \cdots, L$ for an L bit binary sequence emission as shown in Fig. 1. Therein, if Ω_l is a stopband, the conveyed binary data is "1", otherwise "0" for a passband, where $f_{l,1}$ and $f_{l,2}$ denote the lower and upper normalized frequencies associated with Ω_l, respectively.

The communication rate is

$$C_r = Lf_{PRF}. \tag{3}$$

where f_{PRF} is the Pulse Repetition Frequency (PRF).

In the communication receiver, we design a demodulation approach using frequency band energy detection.

III. Problem Formulation

This section focuses on MIMO DFRC waveform formulation through relying on the minimization of ISL in the presence of communication stopband and passband, mainlobe level, PAR and antenna power constraints.

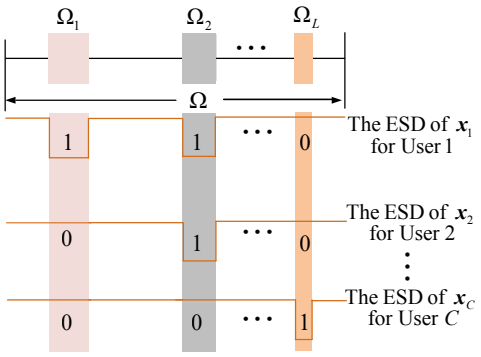

Fig. 1. Information modulation based on the spatio-spectral passbands and stopbands.

A. Waveform Constraints

1) Communication Stopband Constraint: Since we employ the stopband to represent "1", in math, the spectral stopband energy for the c-th user can be expressed as

$$E_{sc} = \sum_{l=1}^{L}\beta_{l,c}\boldsymbol{x}_c^\dagger\boldsymbol{R}_l\boldsymbol{x}_c = \sum_{l=1}^{L}\beta_{l,c}\boldsymbol{a}^T(\varphi_c)\boldsymbol{S}^\dagger\boldsymbol{R}_l\boldsymbol{S}\boldsymbol{a}^*(\varphi_c) \tag{4}$$

where the (m, n)-th entry of $\boldsymbol{R}_l$ is given by [11],

$$\boldsymbol{R}_l(m,n) = \begin{cases}\frac{e^{j2\pi f_{l,2}(m-n)} - e^{j2\pi f_{l,1}(m-n)}}{j2\pi(m-n)}, & m \neq n \\ (f_{l,2} - f_{l,1}), & m = n,\end{cases}$$

$\beta_{l,c} \in \{0, 1\}$ denotes the weighted parameter for the l-th frequency band. In particular, if $\beta_{l,c} = 1$, the binary "1" is embedded, otherwise "0" is delivered. In this respect, the total spectral stopband energy for C users is $E_s = \sum_{c=1}^{C} E_{sc} = \boldsymbol{s}^\dagger\boldsymbol{R}_s\boldsymbol{s}$, where $\boldsymbol{R}_s = \sum_{c=1}^{C}\sum_{l=1}^{L}\beta_{l,c}[\boldsymbol{R}_l^\dagger \otimes (\boldsymbol{a}(\varphi_c)\boldsymbol{a}^\dagger(\varphi_c))]$.

Hence, to achieve the communication, the stopband constraints are required, given by

$$\boldsymbol{s}^\dagger\boldsymbol{R}_s\boldsymbol{s} \leq \eta_s, \tag{5}$$

where η_s is the upper bound of the allowable transmit energy.

2) Communication Passband Constraint: For the purpose of superior reliability of information demodulation, we enforce the spectral passband energy constraint for each user, formulated as

$$\eta_{pc} \leq \boldsymbol{s}^\dagger\boldsymbol{R}_c\boldsymbol{s}, \qquad c = 1, \cdots, C, \tag{6}$$

where η_{pc} is the lower bound of the required transmitting energy for the c-th user and $\boldsymbol{R}_c = \sum_{l=1}^{L} v_{l,c}[\boldsymbol{R}_l^\dagger \otimes (\boldsymbol{a}(\varphi_c)\boldsymbol{a}^\dagger(\varphi_c))]$. In particular, if $v_{l,c} = 1$, the binary "0" is embedded, otherwise "1" is delivered.

B. Waveform Design Problem

To ensure a good MIMO radar beampattern performance while achieving the communication information transmission,

we attempt to maximize 1/ISL with multiple practical constraints, namely,

$$\mathcal{P}_1\begin{cases}\max\limits_{\boldsymbol{s}} & \frac{\boldsymbol{s}^\dagger \boldsymbol{A}_m \boldsymbol{s}}{\boldsymbol{s}^\dagger \boldsymbol{A}_s \boldsymbol{s}} \\ \text{s.t.} & ①\boldsymbol{s}^\dagger \boldsymbol{R}_s \boldsymbol{s} \le \eta_s, \\ & ②\eta_{pc} \le \boldsymbol{s}^\dagger \boldsymbol{R}_c \boldsymbol{s}, c = 1, \cdots, C, \\ & ③P_L - \delta \le \frac{\boldsymbol{s}^\dagger \boldsymbol{A}_k \boldsymbol{s}}{\boldsymbol{s}^\dagger \boldsymbol{A}_0 \boldsymbol{s}} \le P_L + \delta, k = 1, 2, \\ & ④\frac{\max\limits_{m=1,\cdots,M} |\boldsymbol{s}_n(m)|^2}{\frac{1}{M}\|\boldsymbol{s}_n\|^2} \le \gamma, n = 1, \cdots, N, \\ & ⑤\frac{p}{N}(1-\kappa) \le \frac{1}{M}\|\boldsymbol{s}_n\|^2 \le \frac{p}{N}(1+\kappa), n = 1, \cdots, N, \\ & ⑥\frac{1}{M}\|\boldsymbol{s}\|^2 = p. \end{cases}$$

Where $\boldsymbol{A}_s = \frac{1}{M}\sum\limits_{k=1}^{\tilde{K}} \boldsymbol{I}_M \otimes \boldsymbol{a}(\phi_k)\boldsymbol{a}^\dagger(\phi_k)$ and $\boldsymbol{A}_m = \frac{1}{M}\sum\limits_{k=1}^{\hat{K}} \boldsymbol{I}_M \otimes \boldsymbol{a}(\theta_k)\boldsymbol{a}^\dagger(\theta_k)$. $\phi_k, k = 1, \cdots, \tilde{K}$ denote these points in the sidelobe region and $\theta_k, k = 1, \cdots, \hat{K}$ denote these points in the mainlobe region. The constraint ③ is mainlobe width constraint, where $\boldsymbol{A}_k = \frac{1}{M}\boldsymbol{I}_M \otimes \boldsymbol{a}(\theta_k)\boldsymbol{a}^\dagger(\theta_k)$, $\theta_2 - \theta_1$ (with $\theta_2 \ge \theta_0 \ge \theta_1$) denotes the main-beam width, $P_L \in (0, 1)$ and δ is a small positive value. ④ represents PAR constraint where γ controls the maximum allowable PAR on the $\boldsymbol{s}_n$. The last two constraints are power constraints with the overall transmitted power p and a small positive scalar κ. $\mathcal{P}_1$ is a general NP-hard problem due to the non-convexity of both the objective function and the feasible set[1].

In the following section, through an equivalent reformulation of the above non-convex design, a Sequential Block Enhancement (SBE) framework to split the high-dimension problem into multiple low-dimension subproblems with respect to multiple block variables is developed. In each block, an iterative algorithm based on Dinkelbach's procedure [13], Sequential Convex Approximation (SCA) and Interior Point Method [14] (DSIPM), to sequentially tackle a non-convex quadratic problem is proposed.

IV. Hybrid Optimization Technique with SBE-DSIPM For Solving $\mathcal{P}_1$

Before further proceeding, we equivalently transform the above problem into the following problem [15].

$$\mathcal{P}_2\begin{cases}\max\limits_{\boldsymbol{s}} & \frac{\boldsymbol{s}^\dagger \boldsymbol{A}_m \boldsymbol{s}}{\boldsymbol{s}^\dagger \boldsymbol{A}_s \boldsymbol{s}} \\ \text{s.t.} & ①\boldsymbol{s}^\dagger \boldsymbol{R}_s \boldsymbol{s} \le \eta_s, \\ & ②\frac{\eta_{pc}}{Mp} \le \frac{\boldsymbol{s}^\dagger \boldsymbol{R}_c \boldsymbol{s}}{\|\boldsymbol{s}\|^2}, \forall c = 1, \cdots, C, \\ & ③P_L - \delta \le \frac{\boldsymbol{s}^\dagger \boldsymbol{A}_k \boldsymbol{s}}{\boldsymbol{s}^\dagger \boldsymbol{A}_0 \boldsymbol{s}} \le P_L + \delta, k = 1, 2, \\ & ④\frac{\max\limits_{m=1,\cdots,M} |\boldsymbol{s}_n(m)|^2}{\frac{1}{M}\|\boldsymbol{s}_n\|^2} \le \gamma, n = 1, \cdots, N, \\ & ⑤\frac{1}{M}\|\boldsymbol{s}_n\|^2 \le \frac{p}{N}(1+\kappa), n = 1, \cdots, N, \\ & ⑥\frac{1}{N}(1-\kappa) \le \frac{\|\boldsymbol{s}_n\|^2}{\|\boldsymbol{s}\|^2}, n = 1, \cdots, N, \\ & ⑦\frac{1}{Mp}\|\boldsymbol{s}\|^2 \ge 1, \end{cases}$$

[1]The feasible region of $\mathcal{P}_1$ is assumed not empty and a viable methodology namely Feasible Point Pursuit (FPP)-SCA [12] to test the feasible point is adopted.

Next we devise a novel hybrid technique based on SBE-DSIPM to deal with $\mathcal{P}_2$. In particular, an SBE framework to sequentially optimize $(\boldsymbol{s}_1, \cdots, \boldsymbol{s}_N)$ is introduced so as to monotonically improve $f(\boldsymbol{s}_1, \cdots, \boldsymbol{s}_N) = \frac{\boldsymbol{s}^\dagger \boldsymbol{A}_m \boldsymbol{s}}{\boldsymbol{s}^\dagger \boldsymbol{A}_s \boldsymbol{s}}$. Only change in a single component $\boldsymbol{s}_i$ is allowed in finding a new and better solution $(\boldsymbol{s}_1, \cdots, \boldsymbol{s}_N)$ by maximizing $f(\boldsymbol{s}_1, \cdots, \boldsymbol{s}_N)$ at a time. Let $\boldsymbol{s}_n^{(i)}$ denote the i-th solution of the n-th emitting antenna, $n = 1, \cdots, N$. Thereby, at the i-th iteration, it is required to solve orderly the non-convex $\mathcal{P}_{\boldsymbol{s}_n^{(i)}}, n = 1, \cdots, N$, where

$$\mathcal{P}_{\boldsymbol{s}_n^{(i)}}\begin{cases}\max\limits_{\boldsymbol{s}_n} & f(\boldsymbol{s}_n; \bar{\boldsymbol{s}}_{-n}^{(i)}) = \frac{\boldsymbol{s}_n^\dagger \boldsymbol{B}_n \boldsymbol{s}_n + \Re\left\{\boldsymbol{b}_n^\dagger \boldsymbol{s}_n\right\} + b_n}{\boldsymbol{s}_n^\dagger \boldsymbol{W}_n \boldsymbol{s}_n + \Re\left\{\boldsymbol{w}_n^\dagger \boldsymbol{s}_n\right\} + w_n} \\ \text{s.t.} & ①\boldsymbol{s}_n^\dagger \boldsymbol{R}_{sn} \boldsymbol{s}_n + \Re\left\{\boldsymbol{r}_{sn}^\dagger \boldsymbol{s}_n\right\} + r_{sn} \le 0, \\ & ②\bar{\eta}_{pc}(\boldsymbol{s}_n^\dagger \boldsymbol{A}_{cn} \boldsymbol{s}_n + \Re\left\{\boldsymbol{a}_{cn}^\dagger \boldsymbol{s}_n\right\} + a_{cn}) \le \\ & \boldsymbol{s}_n^\dagger \boldsymbol{R}_{cn} \boldsymbol{s}_n + \Re\left\{\boldsymbol{r}_{cn}^\dagger \boldsymbol{s}_n\right\} + r_{cn}, c = 1, \cdots, C, \\ & ③(P_L - \delta)(\boldsymbol{s}_n^\dagger \boldsymbol{A}_{0n} \boldsymbol{s}_n + \Re\left\{\boldsymbol{a}_{0n}^\dagger \boldsymbol{s}_n\right\} + a_{0n}) - \\ & (\boldsymbol{s}_n^\dagger \boldsymbol{A}_{kn} \boldsymbol{s}_n + \Re\left\{\boldsymbol{a}_{kn}^\dagger \boldsymbol{s}_n\right\} + a_{kn}) \le 0, k = 1, 2, \\ & ④(\boldsymbol{s}_n^\dagger \boldsymbol{A}_{kn} \boldsymbol{s}_n + \Re\left\{\boldsymbol{a}_{kn}^\dagger \boldsymbol{s}_n\right\} + a_{kn}) - (P_L + \delta) \times \\ & (\boldsymbol{s}_n^\dagger \boldsymbol{A}_{0n} \boldsymbol{s}_n + \Re\left\{\boldsymbol{a}_{0n}^\dagger \boldsymbol{s}_n\right\} + a_{0n}) \le 0, k = 1, 2, \\ & ⑤|\boldsymbol{s}_n(m)|^2 - \frac{\gamma}{M}\|\boldsymbol{s}_n\|^2 \le 0, \forall m, \\ & ⑥\|\boldsymbol{s}_n\|^2 + p_n \le 0, \\ & ⑦ - \|\boldsymbol{s}_n\|^2 + e_n \le 0, \end{cases}$$

where $\boldsymbol{s}^{(n_i)} = \text{vec}([\boldsymbol{s}_1^{(i)}, \cdots, \boldsymbol{s}_{n-1}^{(i)}, \boldsymbol{s}_n, \boldsymbol{s}_{n+1}^{(i-1)}, \cdots, \boldsymbol{s}_N^{(i-1)}]^T) \in \mathbb{C}^{NM}$, $\boldsymbol{s}_{-n}^{(i)} = \text{vec}([\boldsymbol{s}_1^{(i)}, \ldots, \boldsymbol{s}_{n-1}^{(i)}, \boldsymbol{s}_{n+1}^{(i-1)}, \ldots, \boldsymbol{s}_N^{(i-1)}]^T) \in \mathbb{C}^{(N-1)M}$, $\bar{\boldsymbol{s}}_{-n}^{(i)} = \boldsymbol{s}^{(n_i)} - \boldsymbol{\Lambda}_n \boldsymbol{s}_n \in \mathbb{C}^{NM}$, $\boldsymbol{B}_n = \boldsymbol{\Lambda}_n^\dagger \boldsymbol{A}_m \boldsymbol{\Lambda}_n$, $\boldsymbol{b}_n = 2\boldsymbol{\Lambda}_n^\dagger \boldsymbol{A}_m^\dagger \bar{\boldsymbol{s}}_{-n}^{(i)}$, $b_n = \bar{\boldsymbol{s}}_{-n}^{(i)\dagger} \boldsymbol{A}_m \bar{\boldsymbol{s}}_{-n}^{(i)}$, $\boldsymbol{W}_n = \boldsymbol{\Lambda}_n^\dagger \boldsymbol{A}_s \boldsymbol{\Lambda}_n$, $\boldsymbol{w}_n = 2\boldsymbol{\Lambda}_n^\dagger \boldsymbol{A}_s^\dagger \bar{\boldsymbol{s}}_{-n}^{(i)}$, $w_n = \bar{\boldsymbol{s}}_{-n}^{(i)\dagger} \boldsymbol{A}_s \bar{\boldsymbol{s}}_{-n}^{(i)}$, $\boldsymbol{R}_{sn} = \boldsymbol{\Lambda}_n^\dagger \boldsymbol{R}_s \boldsymbol{\Lambda}_n$, $\boldsymbol{r}_{sn} = 2\boldsymbol{\Lambda}_n^\dagger \boldsymbol{R}_s^\dagger \bar{\boldsymbol{s}}_{-n}^{(i)}$, $r_{sn} = \bar{\boldsymbol{s}}_{-n}^{(i)\dagger} \boldsymbol{R}_s \bar{\boldsymbol{s}}_{-n}^{(i)} - \eta_s$, $\boldsymbol{R}_{cn} = \boldsymbol{\Lambda}_n^\dagger \boldsymbol{R}_c \boldsymbol{\Lambda}_n$, $\boldsymbol{r}_{cn} = 2\boldsymbol{\Lambda}_n^\dagger \boldsymbol{R}_c^\dagger \bar{\boldsymbol{s}}_{-n}^{(i)}$, $r_{cn} = \bar{\boldsymbol{s}}_{-n}^{(i)\dagger} \boldsymbol{R}_c \bar{\boldsymbol{s}}_{-n}^{(i)}$, $\boldsymbol{A}_{cn} = \boldsymbol{\Lambda}_n^\dagger \boldsymbol{\Lambda}_n$, $\boldsymbol{a}_{cn} = 2\boldsymbol{\Lambda}_n^\dagger \bar{\boldsymbol{s}}_{-n}^{(i)}$, $a_{cn} = \bar{\boldsymbol{s}}_{-n}^{(i)\dagger} \bar{\boldsymbol{s}}_{-n}^{(i)}$, $\bar{\eta}_{pc} = \eta_{pc}/Mp$, $\boldsymbol{A}_{kn} = \boldsymbol{\Lambda}_n^\dagger \boldsymbol{A}_k \boldsymbol{\Lambda}_n$, $\boldsymbol{a}_{kn} = 2\boldsymbol{\Lambda}_n^\dagger \boldsymbol{A}_k^\dagger \bar{\boldsymbol{s}}_{-n}^{(i)}$, $a_{kn} = \bar{\boldsymbol{s}}_{-n}^{(i)\dagger} \boldsymbol{A}_k \bar{\boldsymbol{s}}_{-n}^{(i)}$, $\boldsymbol{A}_{0n} = \boldsymbol{\Lambda}_n^\dagger \boldsymbol{A}_0 \boldsymbol{\Lambda}_n$, $\boldsymbol{a}_{0n} = 2\boldsymbol{\Lambda}_n^\dagger \boldsymbol{A}_0^\dagger \bar{\boldsymbol{s}}_{-n}^{(i)}$, $a_{0n} = \bar{\boldsymbol{s}}_{-n}^{(i)\dagger} \boldsymbol{A}_0 \bar{\boldsymbol{s}}_{-n}^{(i)}$, $p_n = -\frac{Mp}{N}(1+\kappa)$, $e_{1,n} = \frac{1}{N}(1-\kappa) - 1$, $e_{2,n} = \frac{1}{N}(1-\kappa)\|\boldsymbol{s}_{-n}^{(i)}\|^2$, $e_n = \max\{Mp - \|\boldsymbol{s}_{-n}^{(i)}\|^2, -e_{2,n}/e_{1,n}\}$, and $\boldsymbol{\Lambda}_n \in \mathbb{C}^{NM \times M}$ is given by

$$\boldsymbol{\Lambda}_n(i, \bar{j}) = \begin{cases} 1, & \text{if } i = n + (\bar{j} - 1)N \\ 0, & \text{otherwise} \end{cases}$$

with $i \in \{1, \cdots, NM\}$ and $\bar{j} \in \{1, \cdots, M\}$.

Note that $\mathcal{P}_{\boldsymbol{s}_n^{(i)}}$ is still a non-convex problem. Resorting to the generalized fractional programming theory, we introduce a parameter y for transforming the objective function $f(\boldsymbol{s}_n; \bar{\boldsymbol{s}}_{-n}^{(i)})$ into the following objective function,

$$\chi(y, \boldsymbol{s}_n) = f_0(\boldsymbol{s}_n) - y f_1(\boldsymbol{s}_n),$$

where $f_0(\boldsymbol{s}_n) = \boldsymbol{s}_n^\dagger \boldsymbol{B}_n \boldsymbol{s}_n + \Re\left\{\boldsymbol{b}_n^\dagger \boldsymbol{s}_n\right\} + b_n$ and $f_1(\boldsymbol{s}_n) = \boldsymbol{s}_n^\dagger \boldsymbol{W}_n \boldsymbol{s}_n + \Re\left\{\boldsymbol{w}_n^\dagger \boldsymbol{s}_n\right\} + w_n$. Solving $\mathcal{P}_{\boldsymbol{s}_n^{(i)}}$ can be converted into finding a solution to the following problem:

$$\begin{aligned} \max_{y, \boldsymbol{s}_n} \quad & \chi(y, \boldsymbol{s}_n) \\ \text{s.t.} \quad & \{\boldsymbol{s}_n\} \in \mathcal{S}_n^{(i)} \end{aligned} \tag{7}$$

Now we devote to the solution to Problem (7) invoking Dinkelbach's iterative procedure. In particular, assume the t-th iteration solutions are denoted by $y_{(t)}$ and $\boldsymbol{s}_{n(t)}$, respectively.

1) Given a $\boldsymbol{s}_{n(t-1)}$, $y_{(t)}$= $f_0(\boldsymbol{s}_{n(t-1)})/f_1(\boldsymbol{s}_{n(t-1)})$.
2) Given a $y_{(t)}$, $\boldsymbol{s}_n$ is updated by solving

$$\begin{aligned} \max_{\boldsymbol{s}_n} \quad & \chi(y_{(t)}, \boldsymbol{s}_n) \\ \text{s.t.} \quad & \{\boldsymbol{s}_n\} \in \mathcal{S}_n^{(i)}. \end{aligned} \tag{8}$$

3) Repeat the above procedures until convergence.

However, Problem (8) is still difficult to solve because of the non-convex constraints and non-concave objective function. Now we approximately deal with it leveraging SCA via its convex version using the following proposition. Problem (8) with respect to $\boldsymbol{s}_n$ can be approximately tackled via a convex problem $\mathcal{P}_{\boldsymbol{s}_{n(t)}}$

$$\mathcal{P}_{\boldsymbol{s}_{n(t)}} \begin{cases} \max\limits_{\boldsymbol{s}_n} & \boldsymbol{s}_n^\dagger \boldsymbol{D}_n \boldsymbol{s}_n + \Re\left\{\boldsymbol{d}_n^\dagger \boldsymbol{s}_n\right\} + d_n \\ \text{s.t.} & \boldsymbol{s}_n^\dagger \boldsymbol{R}_{sn} \boldsymbol{s}_n + \Re\left\{\boldsymbol{r}_{sn}^\dagger \boldsymbol{s}_n\right\} + r_{sn} \le 0, \\ & \boldsymbol{s}_n^\dagger \bar{\boldsymbol{R}}_{cn} \boldsymbol{s}_n + \Re\left\{\bar{\boldsymbol{r}}_{cn}^\dagger \boldsymbol{s}_n\right\} + \\ & \bar{r}_{cn} \le 0, c = 1, \ldots, C, \\ & \boldsymbol{s}_n^\dagger \bar{\boldsymbol{A}}_{kn} \boldsymbol{s}_n + \Re\left\{\bar{\boldsymbol{a}}_{kn}^\dagger \boldsymbol{s}_n\right\} + \\ & \bar{a}_{kn} \le 0, k = 1, 2, \\ & \boldsymbol{s}_n^\dagger \tilde{\boldsymbol{A}}_{kn} \boldsymbol{s}_n + \Re\left\{\tilde{\boldsymbol{a}}_{kn}^\dagger \boldsymbol{s}_n\right\} + \\ & \tilde{a}_{kn} \le 0, k = 1, 2, \\ & |\boldsymbol{s}_n(m)|^2 + \Re\left\{\boldsymbol{q}_n^\dagger \boldsymbol{s}_n\right\} + q_n \le 0, \\ & m = 1, \cdots, M, \\ & \|\boldsymbol{s}_n\|^2 + p_n \le 0, \\ & \Re\left\{\bar{\boldsymbol{q}}_n^\dagger \boldsymbol{s}_n\right\} + \bar{q}_n \le 0, \end{cases}$$

where $\boldsymbol{D}_n = -y_{(t)}\boldsymbol{W}_n$, $\boldsymbol{d}_n = -y_{(t)}\boldsymbol{w}_n + 2\boldsymbol{B}_n \boldsymbol{s}_{n(t-1)} + \boldsymbol{b}_n$, $d_n = -y_{(t)} w_n - \boldsymbol{s}_{n(t-1)}^\dagger \boldsymbol{B}_n \boldsymbol{s}_{n(t-1)} + b_n$.If constraints ②,③ and ④ in $\mathcal{P}_{\boldsymbol{s}_{n(t)}}$ are not approximated, then $\bar{\boldsymbol{R}}_{cn} = \bar{\eta}_{pc}\boldsymbol{A}_{cn} - \boldsymbol{R}_{cn}$, $\bar{\boldsymbol{A}}_{kn} = (P_L - \delta)\boldsymbol{A}_{0n} - \boldsymbol{A}_{kn}$, $\tilde{\boldsymbol{A}}_{kn} = \boldsymbol{A}_{kn} - (P_L + \delta)\boldsymbol{A}_{0n}$, $\bar{\boldsymbol{r}}_{cn} = \bar{\eta}_{pc}\boldsymbol{a}_{cn} - \boldsymbol{r}_{cn}$, $\bar{\boldsymbol{a}}_{kn} = (P_L - \delta)\boldsymbol{a}_{0n} - \boldsymbol{a}_{kn}$, $\tilde{\boldsymbol{a}}_{kn} = \boldsymbol{a}_{kn} - (P_L + \delta)\boldsymbol{a}_{0n}$, $\bar{r}_{cn} = \bar{\eta}_{pc} a_{cn} - r_{cn}$, $\bar{a}_{kn} = (P_L - \delta)a_{0n} - a_{kn}$ and $\tilde{a}_{kn} = a_{kn} - (P_L + \delta)a_{0n}$. Otherwise, $\bar{\boldsymbol{R}}_{cn} = \bar{\eta}_{pc}\boldsymbol{A}_{cn}$, $\bar{\boldsymbol{A}}_{kn} = (P_L - \delta)\boldsymbol{A}_{0n}$, $\tilde{\boldsymbol{A}}_{kn} = \boldsymbol{A}_{kn}$, $\bar{\boldsymbol{r}}_{cn} = \bar{\eta}_{pc}\boldsymbol{a}_{cn} - \boldsymbol{r}_{cn} - 2\boldsymbol{R}_{cn}\boldsymbol{s}_{n(t-1)}$, $\bar{\boldsymbol{a}}_{kn} = (P_L - \delta)\boldsymbol{a}_{0n} - \boldsymbol{a}_{kn} - 2\boldsymbol{A}_{kn}\boldsymbol{s}_{n(t-1)}$, $\tilde{\boldsymbol{a}}_{kn} = \boldsymbol{a}_{kn} - (P_L + \delta)(2\boldsymbol{A}_{0n}\boldsymbol{s}_{n(t-1)} + \boldsymbol{a}_{0n})$, $\bar{r}_{cn} = \bar{\eta}_{pc} a_{cn} - r_{cn} + \boldsymbol{s}_{n(t-1)}^\dagger \boldsymbol{R}_{cn}\boldsymbol{s}_{n(t-1)}$, $\bar{a}_{kn} = (P_L - \delta)a_{0n} - a_{kn} + \boldsymbol{s}_{n(t-1)}^\dagger \boldsymbol{A}_{kn}\boldsymbol{s}_{n(t-1)}$ and $\tilde{a}_{kn} = a_{kn} - (P_L + \delta)(a_{0n} - \boldsymbol{s}_{n(t-1)}^\dagger \boldsymbol{A}_{0n}\boldsymbol{s}_{n(t-1)})$, $\boldsymbol{q}_n = -\frac{\gamma}{M} 2\boldsymbol{s}_{n(t-1)}$, $q_n = \frac{\gamma}{M}\boldsymbol{s}_{n(t-1)}^\dagger \boldsymbol{s}_{n(t-1)}$, and $\bar{\boldsymbol{q}}_n = -2\boldsymbol{s}_{n(t-1)}$, $\bar{q}_n = \boldsymbol{s}_{n(t-1)}^\dagger \boldsymbol{s}_{n(t-1)} + e_n$.

Finally, we simply use the Interior Point Method that can solve the convex problem $\mathcal{P}_{\boldsymbol{s}_{n(t)}}$.

V. Numerical Results

This section evaluates the performance of the proposed algorithm in terms of the achievable beampattern and reliability of communication. We consider a uniform linear transmit array consisting of $N = 8$ antennas with spaced half wavelength apart. The number of the waveform sample is assumed $M = 32$ and the parameters of power constraints are set to $p = 1$ and $\kappa = 0.5$. The parameters of mainlobe width constraints are supposed to $\theta = 0°$, $\theta_1 = -8°$, $\theta_2 = 8°$, $P_L = 0.5$ and $\delta = 0.05$. We further assume that the communication information is embedded in 9 normalized frequency bands, i.e., $\Omega_1 = [0.1, 0.13]$, $\Omega_2 = [0.2, 0.23]$, $\Omega_3 = [0.3, 0.33]$, $\Omega_4 = [0.4, 0.43]$, $\Omega_5 = [0.5, 0.53]$, $\Omega_6 = [0.6, 0.63]$, $\Omega_7 = [0.7, 0.73]$, $\Omega_8 = [0.8, 0.83]$ and $\Omega_9 = [0.9, 0.93]$. In one radar pulse, two independent sequences 010101101 and 110001001 are transmitted to two communication receivers located in directions $\varphi_1 = 60°$ and $\varphi_2 = -70°$, respectively. The sidelobe region is set to $[-90°, -10°] \bigcup [10°, 90°]$. Unless otherwise stated, the stopband frequency band energy is $\eta_s = 2.5 \times 10^{-5} \times n_s$ where n_s denotes the number of stopband for all communication users. $\eta_p = \eta_{pc}/n_{pc}$, n_{pc} denotes the number of passband for the c-th communication user. The exit conditions are considered as 10^{-2} and 10^{-4} in Dinkelbach's procedure and SBE framework, respectively.

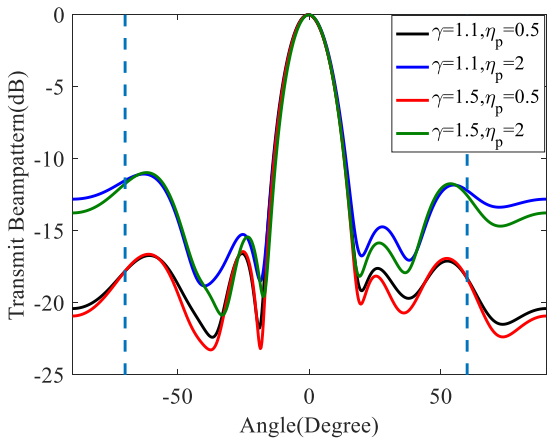

Fig. 2. Beampattern versus angle for $\gamma = 1.1, 1.5$ and $\eta_p = 0.5, 2$.

A. Beampattern Performance

In this subsection, we discuss the optimized beampattern performance for different γ and η_p values. In Fig. 2, the resulting normalized beampatterns obtained via the mentioned algorithms are depicted for $\eta_p = 0.5, 2$ with $\gamma = 1.1, 1.5$.

Inspection of Fig. 2 reveals that, all optimized beampatterns have the high sidelobe level around directions in communication users (i.e., $\varphi_1 = 60°$ and $\varphi_2 = -70°$). This is due to the fact that more waveform energy is required to transmit to communication user through setting suitable η_p value. Besides, it is clearly observed that the smaller the η_p value and the larger the γ value, the better beampattern performance. From the hardware's implementation view, a large γ value will severely impairing the waveform fidelity when the radar amplifier works in near saturation region. As a result, a suitable γ performs a trade-off between beampattern performance and the waveform distortion.

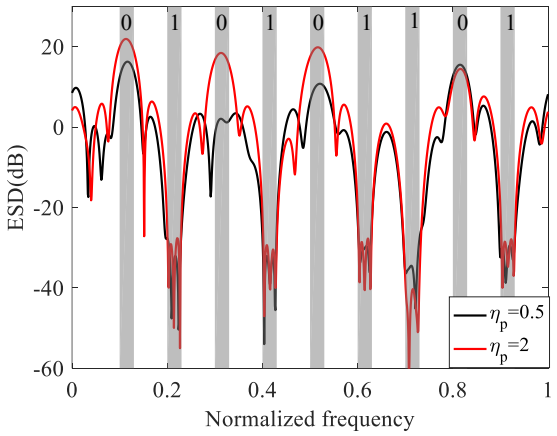

Fig. 3. The optimized ESDs for communication user 1 assuming $\gamma = 1.1$ and $\eta_p = 0.5, 2$.

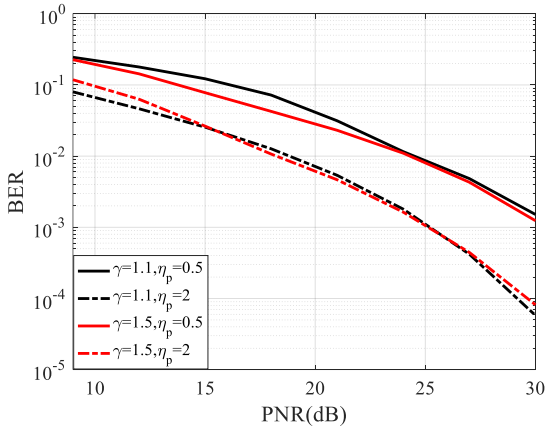

Fig. 4. BER versus PNR for communication user1 assuming $\gamma = 1.1, 1.5$ and $\eta_p = 0.5, 2$.

B. Communication Performance

This subsection focuses on the communication performance considering Bit Error Ratio (BER) metric. According to the based band echo $\tilde{\boldsymbol{x}}_c \in \mathbb{C}^{M\times 1}$ in (2), the Power Noise Ratio (PNR) for received by the c-th user is defined as $|\beta_c|^2/\sigma_c^2$.

Fig. 3 delineates the optimized ESDs (in dB) towards to two communication users located in directions $\varphi_1 = 60^\circ$ for $\eta_p = 0.5, 2$ with fixed $\gamma = 1.1$. Clearly, larger passband energy is achieved with increasing η_p as required by the imposed passpand spectral constraints.

The BERs versus the PNR (in dB) for communication user1 with $\eta_p = 0.5, 2$ and $\gamma = 1.1, 1.5$ is shown in Fig. 4. It is clearly seen that a larger η_p provides superior BER performance as more energy is transmitted to communication users which actually is equivalent to increasing PNR. However, different γ values almost cannot bring any effect on the BER because it does not control the shape of ESDs. Finally, looking over Figs. 2 and 4 reveals that a suitable η_p should be selected carefully to fulfill beampattern performance and BER requirement.

VI. Conclusions

In this paper, we have proposed a novel integrated waveform design method in MIMO DFRC system. A desired radar beampattern and multi-users communication are implemented simultaneously associated with spatio-spectral stopband and passband, PAR, mainlobe width and power constraints. We have also proposed a SBE-DSIPM method to monotonically decrease the beampattern ISL where the Dinkelbach's procedure, SCA and IPM have been introduced in each block. Numerical simulation results have shown that the designed integrated waveform is able to achieve dual function simultaneously.

References

[1] A. Hassanien, M. G. Amin, E. Aboutanios, and B. Himed, "Dual-function radar communication systems: a solution to the spectrum congestion problem," *IEEE Signal Process. Mag.* , vol. 36, no. 5, pp. 115–126, Sep. 2019.

[2] G. Cui, J. Yang, S. Lu, X. Yu, and L. Kong, "Dual-use unimodular sequence design via frequency nulling modulation," *IEEE Access*, vol. 6, pp. 62470– 62481, 2018

[3] J. Yang, G. Cui, X. Yu, and L. Kong, "Dual-use signal design for radar and communication via ambiguity function sidelobe control," *IEEE Trans. Veh. Technol.*, vol. 69, no. 9, pp. 9781–9794, Sep. 2020.

[4] A. Hassanien, M. G. Amin, Y. D. Zhang and F. Ahmad, "Dual-function radar-communications: information embedding using sidelobe control and waveform diversity," *IEEE Trans. Signal Process.*, vol. 64, no. 8, pp. 2168–2181, Apr. 2016.

[5] A. Hassanien, M. G. Amin, Y. D. Zhang and F. Ahmad, "Phase-modulation based dual-function radar-communications," *IET Radar, Sonar, Navig.*, vol. 10, no. 8, pp. 1411–1421, Oct. 2016.

[6] T. Huang, N. Shlezinger, X. Xu, Y. Liu and Y. C. Eldar, "MAJoRCom: a dual-function radar communication system using index modulation," *IEEE Trans. Signal Process.*, vol. 68, pp. 3423–3438, May. 2020.

[7] X. Wang, A. Hassanien and M. G. Amin, "Dual-function MIMO radar communications system design via sparse array optimization," *IEEE Trans. Aerosp. Electron. Syst.*, vol. 55, no. 3, pp. 1213–1226, Jun. 2019.

[8] X. Wang and A. Hassanien, "Phase modulated communications embedded in correlated FH-MIMO radar waveforms," in *IEEE Radar Conference*, Florence, Italy, pp. 1–6, Sep. 2020.

[9] X. Wang, J. Xu, A. Hassanien, and E. Aboutanios, "Joint communications with FH-MIMO Radar systems: an extended signaling strategy," in *2021 IEEE International Conference on Acoustics, Speech and Signal Processing*, Toronto, ON, Canada, pp. 8253–8257, Jun. 2021.

[10] F. Liu, C. Masouros, T. Ratnarajah, and A. Petropulu, "On range sidelobe reduction for dual-functional radar-communication waveforms," *IEEE Wireless Commun. Lett.*, vol. 9, no. 9, pp. 1572–1576, Sep. 2020.

[11] A. Aubry, A. De Maio, M. Piezzo, and A. Farina, "Radar waveform design in a spectrally crowded environment via nonconvex quadratic optimization," *IEEE Trans. Aerosp. Electron. Syst.*, vol. 50, no. 2, pp. 1138–1152, 2014.

[12] O. Mehanna, K. Huang, B. Gopalakrishnan, A. Konar, and N. D. Sidiropoulos, "Feasible point pursuit and successive approximation of non-convex QCQPs", *IEEE Signal Process Lett.*, vol. 22, no. 7, pp. 804–808, Jul. 2015.

[13] J. P. Crouzeix, J. A. Ferland and S. Schaible, "An algorithm for generalized fractional programs," *J. Optim. Theory Appl.*, vol. 47, no. 8, pp. 35-49, Sep. 1985.

[14] S. Boyd and L. Vandenberghe, Convex Optimization. Cambridge Univ. Press., 2004.

[15] X. Yu, H. Qiu, J. Yang, W. Wei, G. Cui, L. Kong, "Multi-Spectrally constrained MIMO radar beampattern design via sequential convex approximation," *IEEE Trans. Aerosp. Electron. Syst.*, Feb. 2022.